

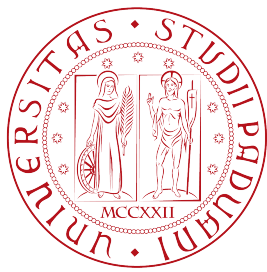
UNIVERSITÀ DEGLI STUDI DI PADOVA
DEPARTMENT OF INFORMATION ENGINEERING
Master Thesis in Telecommunication Engineering

DESIGN OF REAL-TIME OPTICAL COHERENCE
TOMOGRAPHY

Master Candidate
GIANLUCA MARCON

Supervisor
LUCA PALMIERI

April 18, 2018
Academic Year 2017/2018



UNIVERSITÀ DEGLI STUDI DI PADOVA
DEPARTMENT OF INFORMATION ENGINEERING
Master Thesis in Telecommunication Engineering

DESIGN OF REAL-TIME OPTICAL COHERENCE
TOMOGRAPHY

Master Candidate
GIANLUCA MARCON

Supervisor
LUCA PALMIERI

April 18, 2018
Academic Year 2017/2018

Gianluca Marcon: *Design of Real-Time Optical Coherence Tomography*,
Master Thesis in Telecommunication Engineering ©, Department of
Information Engineering, Università degli Studi di Padova, April
2018

ABSTRACT

OCT! (**OCT!**) is a non-invasive imaging technique that exploits the coherence property of light to generate 2-D (cross-sectional) and 3-D (volumetric) images of a live sample from the backscattered electromagnetic field. OCT imaging has found widespread application in medicine, mainly in the areas of *Ophthalmology* and *Angiography*, but also in industrial processes where non-destructive or contactless testing is necessary.

There are two main categories of OCT systems: **TD-OCT!** (**TD-OCT!**) and **FD-OCT!** (**FD-OCT!**). As the names suggest, the former technique makes use of time domain measurements, while the latter takes advantage of the frequency contents of the reflected signals. FD-OCT offers significant advantages over TD-OCT, such as faster scanning rates, better imaging resolution, and enhanced sensitivity, while at the same time requiring no mechanical movements of critical components such as lenses or collimators.

In this thesis I focus on a particular FD-OCT technique called **SS-OCT!** (**ss-OCT!**), which uses a rapidly tunable narrow band laser as a light source. A working SS-OCT system capable of real-time imaging is fully developed, along with the data-acquisition and signal-processing modules needed for a complete tomographic imaging device.

Future development includes the migration of the signal processing stack on a **GPU!** (**GPU!**) in order to enhance the performance of the system making use of the **GPGPU!** (**GPGPU!**) paradigm. This approach opens up the possibility to implement more advanced and refined OCT schemes, such as **PS-OCT!** (**ps-OCT!**) and **svOCT!** (**svOCT!**).

SOMMARIO

La Tomografia a Coerenza Ottica (**OCT!**) è una tecnica di imaging non invasiva che sfrutta la proprietà di coerenza della luce per generare immagini 2-D (a sezioni) e 3-D (volumetriche) di un campione in vivo a partire dalla luce retrodiffusa dallo stesso. La tecnica OCT ha trovato ampio utilizzo nel campo della medicina, in particolare nelle aree dell'*Oftalmologia* e dell'*Angiografia*, ma anche in processi industriali in cui sono necessarie misure non distruttive e senza contatto.

Vi sono due principali categorie di sistemi OCT: TD-OCT (OCT nel dominio del tempo) e FD-OCT (OCT nel dominio della frequenza). Come suggerisce il nome, la prima di queste due tecniche sfrutta delle misure nel dominio del tempo, mentre la seconda utilizza il contenuto spettrale dei segnali riflessi per ricostruire l'immagine del campione in esame. FD-OCT offre vantaggi significativi rispetto a TD-OCT, come velocità di scansione più elevate, risoluzione più fine e migliore sensitività. Tutto ciò avviene senza che vi siano movimenti meccanici di componenti critici come lenti e collimatori.

In questa tesi lavorerò su un particolare sistema FD-OCT chiamato Swept-Source OCT (**ss-OCT!**) che sfrutta un laser a banda molto stretta e con alta velocità di sintonizzazione. Verrà quindi sviluppato un sistema SS-OCT funzionante, capace di eseguire misure continue e in tempo reale. Il lavoro verterà sulla parte di progettazione e ottimizzazione dello schema ottico e sullo sviluppo di algoritmi per l'acquisizione ed elaborazione dei dati.

Sviluppi futuri verteranno sulla migrazione dell'intero sistema di elaborazione dati su GPU (Graphical Processing Unit) facendo uso del paradigma di **GPGPU!** (**GPGPU!**), che renderà più efficiente il dispositivo e permetterà la progettazione di tecniche più avanzate come OCT sensibile alla polarizzazione (**PS-OCT!**), per ottenere misure di birifrangenza del campione, o **svOCT!** (**svOCT!**).

INTRODUCTION

1.1 SUMMARY ON OPTICAL COHERENCE TOMOGRAPHY

The technique of **OCT!** (**OCT!**), firstly introduced in the late 80's by Fujimoto et al. [11] and later improved by Huang et al. [14], was developed for the noninvasive axial and cross-sectional imaging of biological tissues. In a way similar to ultrasonic imaging, 2D images are generated by combining the incident electromagnetic radiation with its delayed version reflected by the sample under test.

The advantage over conventional ultrasound techniques is that it permits imaging resolutions that range from 1 to 20 μm , which is up to two orders of magnitude smaller than for ultrasound. This enables the diagnosis of pathologies which were previously only detectable by histological techniques, which have the advantage of higher resolution at the expense of the capability of non-destructive measurement. In fact, histology requires the following steps to be performed on the sample:

- Excision
- Fixation
- Embedding
- Microtoming
- Staining

These operations prevent the use of histology in certain areas where the sample to be analyzed cannot be damaged, such as *Ophthalmology*, a field of medicine which studies the pathologies of the human eyeball and orbit. These characteristics, coupled with its real-time imaging capability, makes **OCT!** one of the strongest candidates for this particular branch of medicine. In [Figure 1.1](#) we can compare the images of a human retina obtained from TD-OCT ([Figure 1.1a](#)) and histology ([Figure 1.1b](#)) [14]. Image quality, while arguably low, is enough to identify and measure the thickness of the main structures of the eye. In [Figure 1.1c](#) we can instead see a high quality image of a live sample obtained with the **SS-OCT!** (**ss-OCT!**) technique [8].

The first drawback of OCT as a medical imaging technique comes from its relatively low imaging penetration, which is usually between less than a millimeter up to a couple of centimeter, depending on the

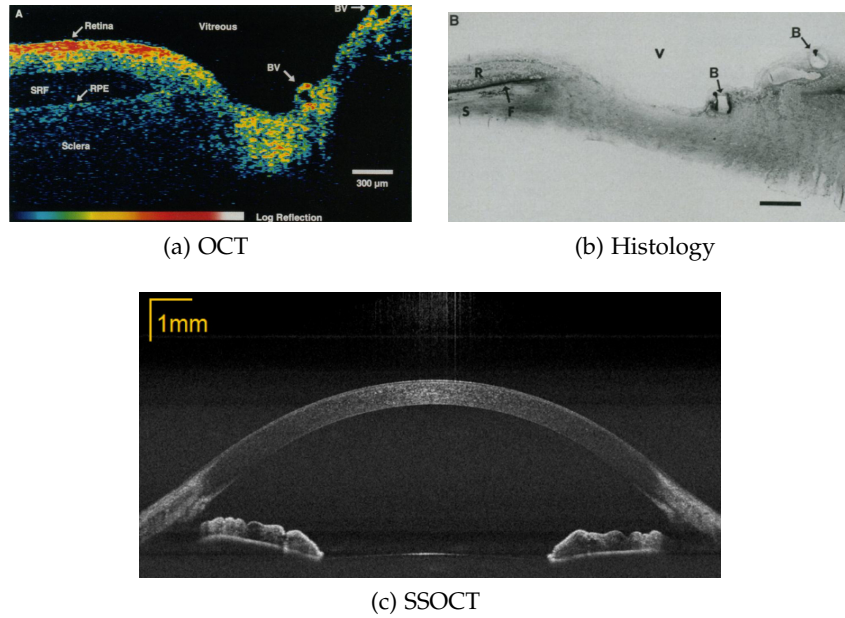


Figure 1.1: Optical coherence tomograph of human retina and optic disk in vitro (top left) and histologic section of the same sample (top right) [14]. On the bottom, a ss-OCT! image of a live human eye sample [8].

specific technology and the absorption coefficient of the sample to analyse. In Figure 1.2, a comparison between OCT, Ultrasound, and Confocal Microscopy is available [9]. The trend is that for an increasingly better imaging resolution, imaging depth has to be sacrificed. In this aspect, OCT sits right between the other two techniques, offering micrometer-level resolution for a moderate image penetration.

When cross-sectional images are not sufficient for a correct diagnosis, volumetric data can be exploited for a more in-depth analysis. Two examples of 3D-OCT data obtained with SS-OCT (left) [8] and SD-OCT (right) [6] are depicted in Figure 1.3. With the near-exponential growth in computing power over the last decades, and

SOURCE	YEAR	VOXELS	VOL. RATE	SPEED
			Volumes/s	GVoxels/s
Zhang and Kang[26]	2010	6400000	10	0.06
Choi et al. [6]	2012	4194304	41	0.17
Wieser et al. [24]	2014	40960000	26	1.07
Darbrazi [7]	2016	1408800000	2.05	2.89

Table 1.1: Performance of different implementations of volumetric OCT using GPGPU (adapted from [7]).

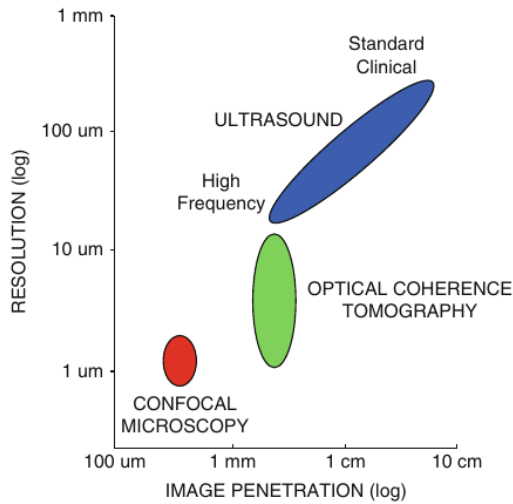


Figure 1.2: Imaging resolution and image penetration compared for different imaging techniques.

the advent of GPU! computing by means of the GPGPU! paradigm, advanced volume rendering and signal-processing algorithms can be applied on large OCT data sets in real-time, breaking the 1 GigaVoxel/second mark. In Table 1.1 a few results from the literature are summarized, highlighting the advancement in processing power using GPU solutions (adapted from [7]).

A voxel is the primary unit of three-dimensional datasets, like the pixel is for 2D data

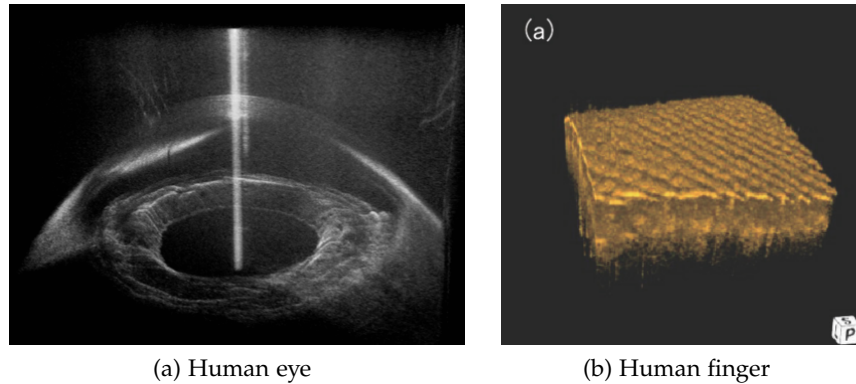


Figure 1.3: Example of 3D OCT data: human eye obtained with SS-OCT [8] (left) and human finger obtained with SD-OCT [6] (right).

1.2 APPLICATIONS

1.2.1 Endoscopy

Ophtalmic applications have already been briefly mentioned in Section 1.1, but other areas of medicine such as Cardiology[4, 15] and Angiography[16, 22] have benefitted from the diagnostic capability

of OCT. A comparison between OCT and Ultrasound images of a coronary plaque is available in [Figure 1.5](#): the higher resolution of the optical system is substantial. These applications are made possible by the small footprint of optical fibers (in the order of $200\text{ }\mu\text{m}$ of diameter), which can be easily embedded in endoscopes, catheters or other special probes [19, 23]. An example of a focus-adjustable probe is depicted in [Figure 1.4](#). A OCT system can then be divided into an imaging engine consisting of optical source, circulators and other fiber-optic based components, and a separate imaging device, specific to the application. EOCT! (EOCT!) thus an important tool for the detection of cancers affecting different parts of the human body, including bladder [25], cervix [10] and colon [13]. Other applications in the field of medicine include dermatology and skin damage assessment [12, 17], dentistry [1, 20]

Angiography or arteriography is a medical imaging technique used to visualize the inside, or lumen, of blood vessels and organs of the body

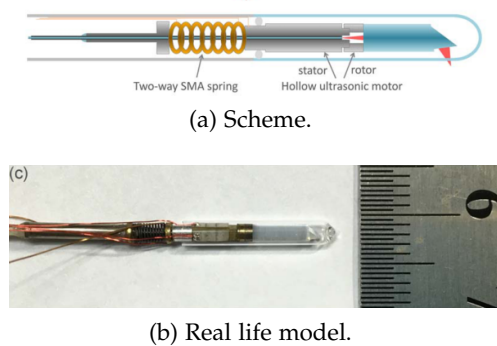


Figure 1.4: Probe for endoscopic OCT [19].

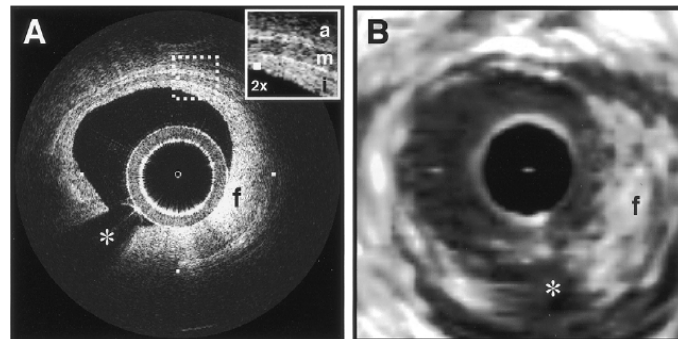


Figure 1.5: Coronary plaque imaged by OCT (left) and intravascular ultrasound (IVUS) (right) [15].

1.3 OBJECTIVES

Expand on Calabrese[5]

1.4 THESIS STRUCTURE

2

BASIC THEORY OF OPTICAL COHERENCE TOMOGRAPHY

In this chapter I will report the basic theoretical background needed to comprehend the working mechanisms behind the OCT technique, introduce the different schemes and compare them in terms of performance. A brief description of the main areas of application will also be given.

2.1 PRINCIPLES OF COHERENCE AND INTERFERENCE

Copy from [3, 21]

2.1.1 *Interference*

2.1.2 *Temporal Coherence*

2.1.3 *Spatial Coherence*

2.2 DESCRIPTION OF VARIOUS OCT TECHNIQUES

Make examples of laser sources for each category, technology used citing recent articles. Make sure to talk about the compensation needed in case of SSOCT and SDOCT and how to solve it, both in hardware and post processing.

2.2.1 *Terminology*

2.2.2 *Time Domain OCT*

Insert picture of basic Michelson interferometer and expand on that. Show axial measurements of rabbit eye and whatnot.

2.2.3 *Frequency Domain OCT*

Spectral Domain OCT

How it works, laser sources, compensation, camera receiver...

Swept-Source OCT

Explain in detail. Make graph of frequency vs time, maybe take it from [9]

$$f(t) = A \exp(j2\pi f_1 t) + B \exp(j2\pi f_2 t), \quad f_1 \neq f_2 \quad (2.1)$$

$$i(t) \propto f(t)f^*(t) = A + B + 2AB\Re\{\exp[2\pi(f_1 - f_2)t]\} \quad (2.2)$$

$$\propto \cos(2\pi\Delta ft). \quad (2.3)$$

2.3 APPLICATIONS OF OCT

2.3.1 Medicine

2.3.2 Industrial

2.3.3 Guided Microsurgery

2.4 A NEW SECTION

Examples: *Italics*, ALL CAPS, SMALL CAPS, LOW SMALL CAPS¹. Acronym testing: UML! (UML!) – UML! – UML! (UML!) – UML!s – OCT!

2.4.1 Test for a Subsection

2.4.2 Autem Timeam

Note: The content of this chapter is just some dummy text.

2.5 ANOTHER SECTION IN THIS CHAPTER

DESCRIPTION-LABEL TEST:

LABEL TEST 2:

2.5.1 Personas Initialmente

A Subsubsection

A PARAGRAPH EXAMPLE

2.5.2 Figure Citations

Use i.e. and autoref for citing

¹ Footnote example.

LABITUR BONORUM PRI NO	QUE VISTA	HUMAN
fastidii ea ius	germano	demonstratea
suscipit instructior	titulo	personas
quaestio philosophia	facto	demonstrated [18]

Table 2.1: Autem timeam deleniti usu id. Barajas, Zavareh, and Hoyos

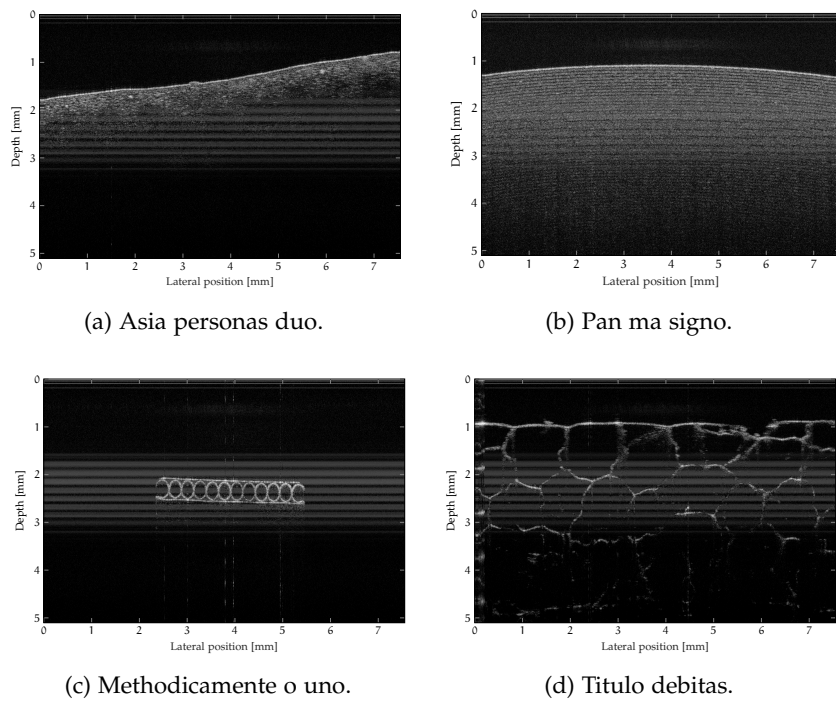


Figure 2.1: Tu duo titulo debitas latente.

DESCRIPTION OF THE SETUP

3.1 OPTICAL DEVICES

3.1.1 *Light Source*

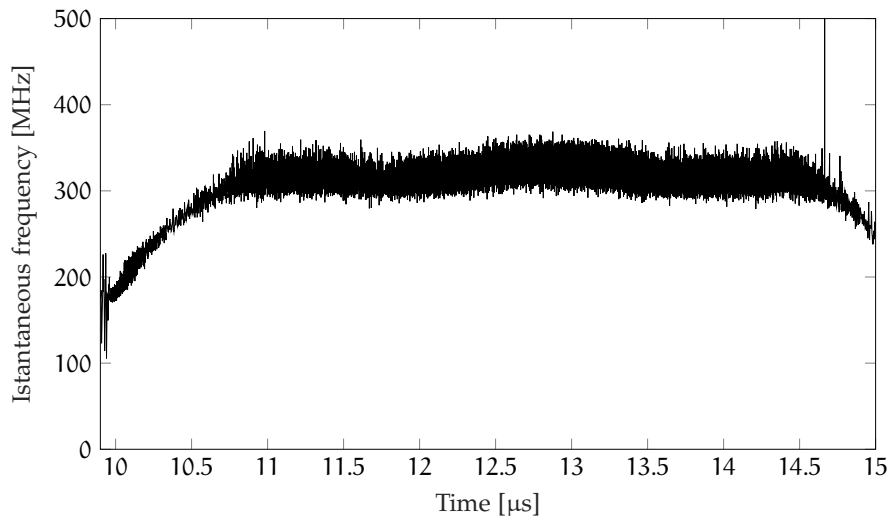


Figure 3.1: Estimate of the instantaneous frequency of the k-clock.

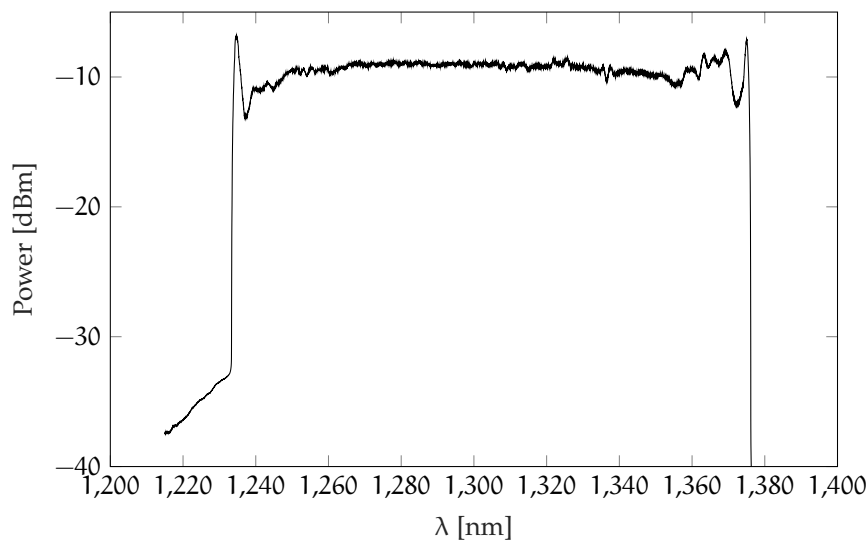


Figure 3.2: Spectrum of the Axsun laser, obtained with a 1 nm resolution.

PARAMETER	UNITS	VALUE
Sweep Rate	kHz	100.2
Center Wavelength	nm	1305
Wavelength Tuning Range	nm	140.38
Average Power	mW	25.7
Duty Cycle	%	77.3
Sampled Duty Cycle	%	50.5
External Clock Min Frequency	MHz	183.1
External Clock Average Frequency	MHz	307.0
External Clock Max Frequency	MHz	332.1
Sampling Clocks	-	1536

Table 3.1: Axsun laser datasheet.

3.1.2 *Couplers*

3.1.3 *Reference Arm*

Collimator calibration

3.1.4 *Sample Arm*

Scanning lens

3.1.5 *Photodiodes*

3.2 GALVANOMETRIC SYSTEM

3.2.1 *Controlling the system*

3.3 ACQUISITION DEVICE

3.3.1

In [Figure 3.4](#) a comparison between the two acquisition techniques is available. For Single-port Acquisitions, in [Figure 3.4b](#) we can see that no trigger events are missed and over 95% of CPU time is available for data processing, while in [Figure 3.4a](#) trigger events happening while the DMA transfer is ongoing are missed completely, and virtually all CPU cycles are used in managing the data acquisition. This leaves no room for data processing on the CPU.



Figure 3.3: The acquisition board, AlazarTech ATS9350.

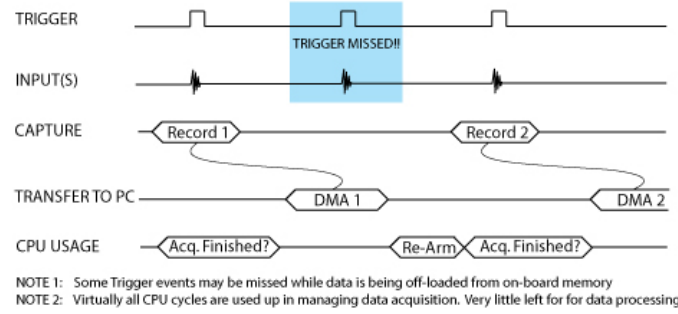
3.4 WORKSTATION

3.5 SOME FORMULAS

z	charge of the incident particle
N_{Av}	Avogadro's number
Z	atomic number of the material
A	atomic weight of the material
ρ	density
δx	thickness of the material

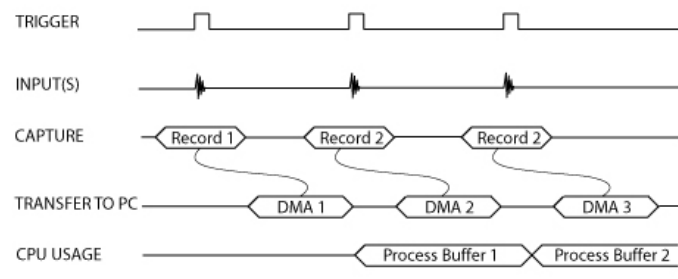
3.6 VARIOUS MATHEMATICAL EXAMPLES

TRIGGERED DATA ACQUISITION USING SINGLE-PORT MEMORY



(a) Acquisition using Single-Port Memory.

TRIGGERED DATA ACQUISITION USING DUAL-PORT MEMORY



(b) Acquisition using Dual-Port Memory.

Figure 3.4: Diagram highlighting the differences between Single-Port acquisitions and Dual-Port acquisitions

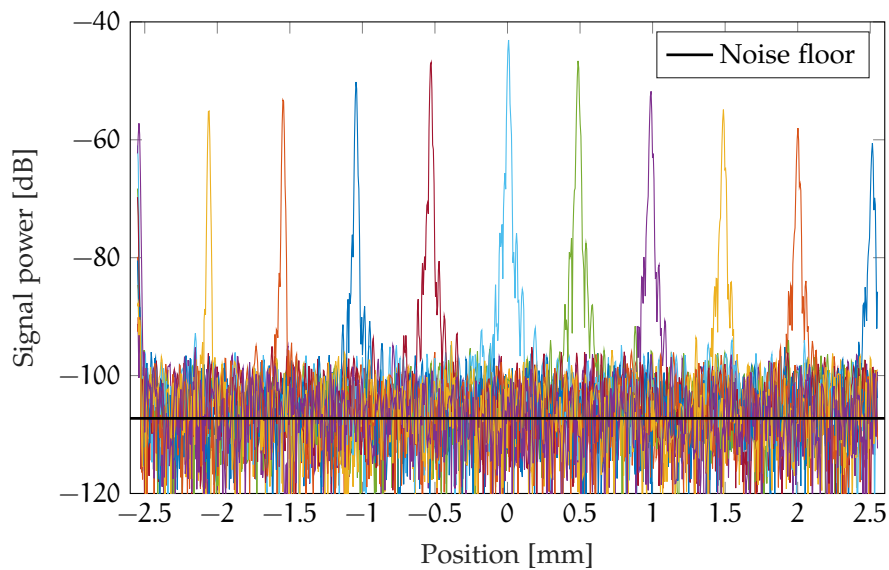


Figure 3.5: Signal spectrum at various depths.

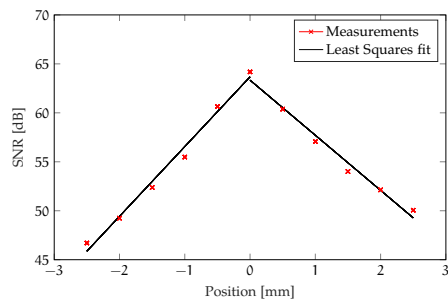


Figure 3.6: Signal-to-noise ratio falloff.

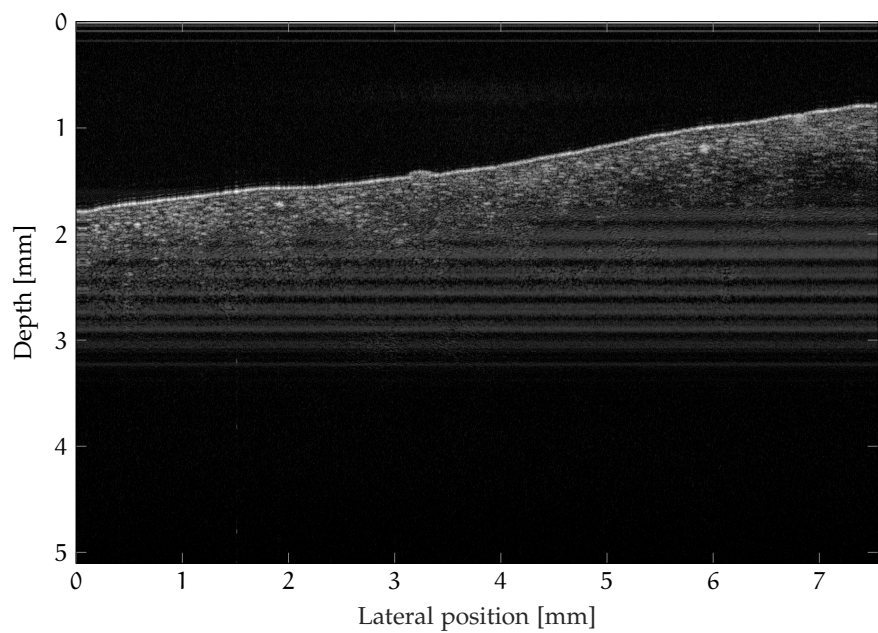


Figure 3.7: B-scan of banana peel.

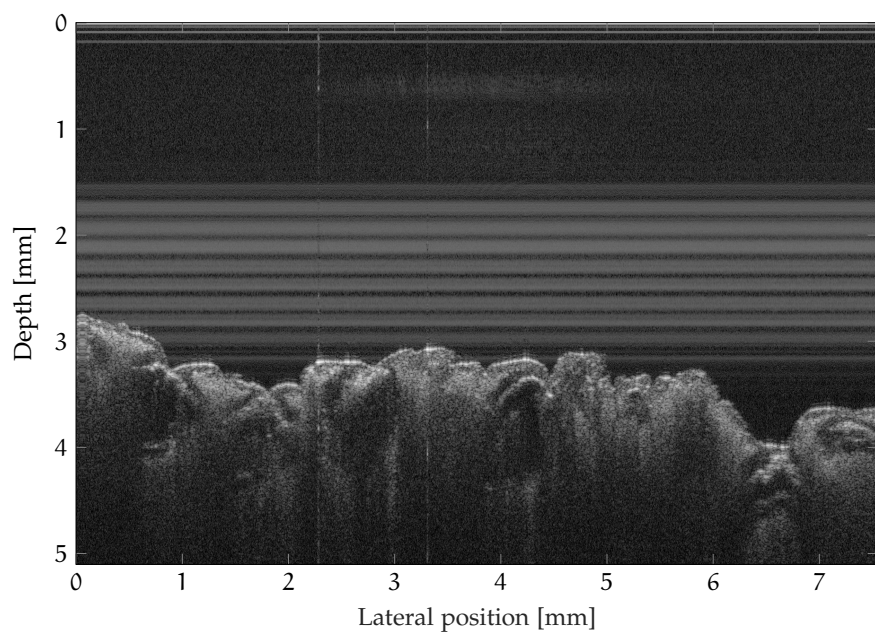


Figure 3.8: B-scan of dry orange peel.

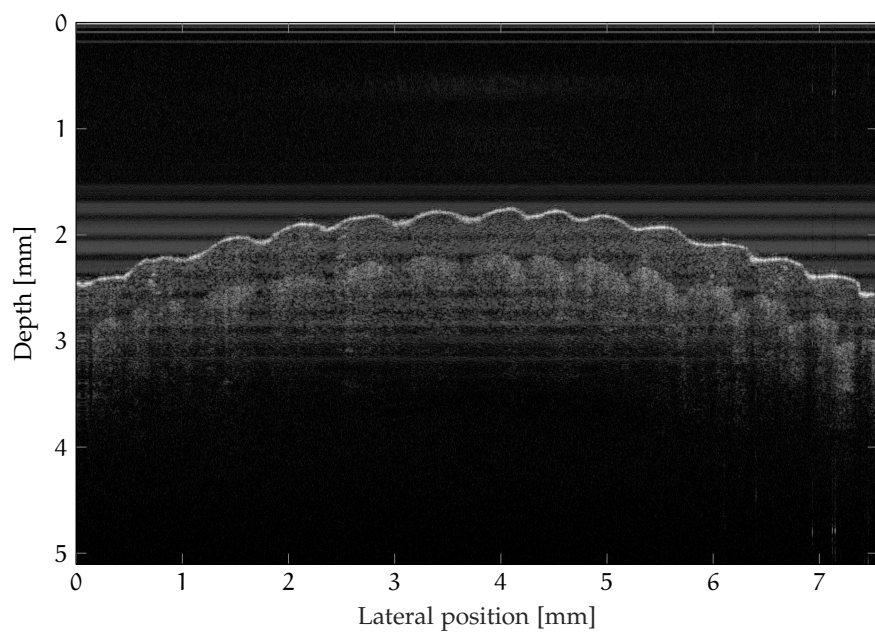


Figure 3.9: B-scan of a human finger.

4

RESULTS

4.1 DATA ACQUISITION SOFTWARE

Lorem ipsum dolor sit amet, consectetuer adipiscing elit. Ut purus elit, vestibulum ut, placerat ac, adipiscing vitae, felis. Curabitur dictum gravida mauris. Nam arcu libero, nonummy eget, consectetuer id, vulputate a, magna. Donec vehicula augue eu neque. Pellentesque habitant morbi tristique senectus et netus et malesuada fames ac turpis egestas. Mauris ut leo. Cras viverra metus rhoncus sem. Nulla et lectus vestibulum urna fringilla ultrices. Phasellus eu tellus sit amet tortor gravida placerat. Integer sapien est, iaculis in, pretium quis, viverra ac, nunc. Praesent eget sem vel leo ultrices bibendum. Aenean faucibus. Morbi dolor nulla, malesuada eu, pulvinar at, mollis ac, nulla. Curabitur auctor semper nulla. Donec varius orci eget risus. Duis nibh mi, congue eu, accumsan eleifend, sagittis quis, diam. Duis eget orci sit amet orci dignissim rutrum.

4.1.1 *Digital Signal Processing Chain for OCT*

4.1.2 *The Qt programming framework*

4.2 THE SIGNAL-SLOT PARADIGM

Blocking vs Non-blocking calls

4.2.1 *Displaying graphics with OpenGL*

4.2.2 *Parallel Computing with OpenMP*

OpenMP¹ is a multi-platform *Application Programming Interface* (API) for shared-memory parallel processing programming available for various programming languages, such as C, C++ and Fortran.

*OpenMP stands for
Open
Multi-Processing*

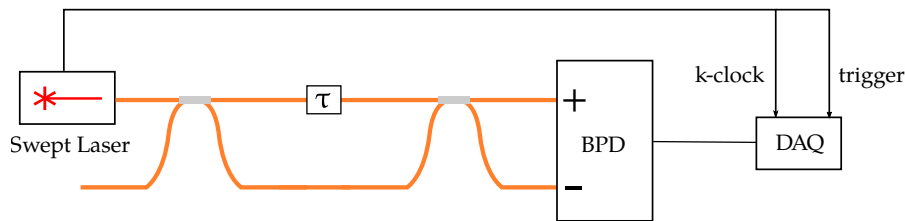


Figure 4.1: Diagram of an unbalanced Mach-Zender Interferometer.

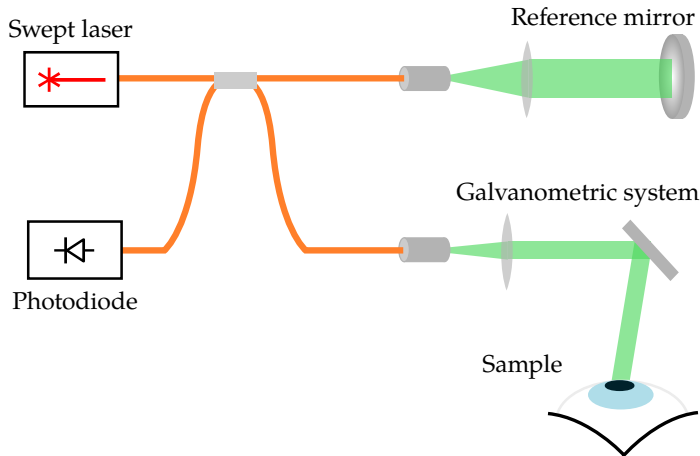


Figure 4.2: Basic diagram of a SS-OCT setup

4.2.3 *Mach-Zender Interferometer*

4.3 BASIC SETUP

Stability Analysis

4.3.1 *New setup*

4.3.2 *Balancing the optical paths*

Working mechanism of a OBR

Measuring path lengths

4.3.3 *Axial Resolution*

resolution = minimum distance at which two objects are distinguishable NOT absolute position of an object. Also explain that worse result than theoretical might be explained by dispersion in the system and the use of a SMF patch cord designed for 1550nm range.

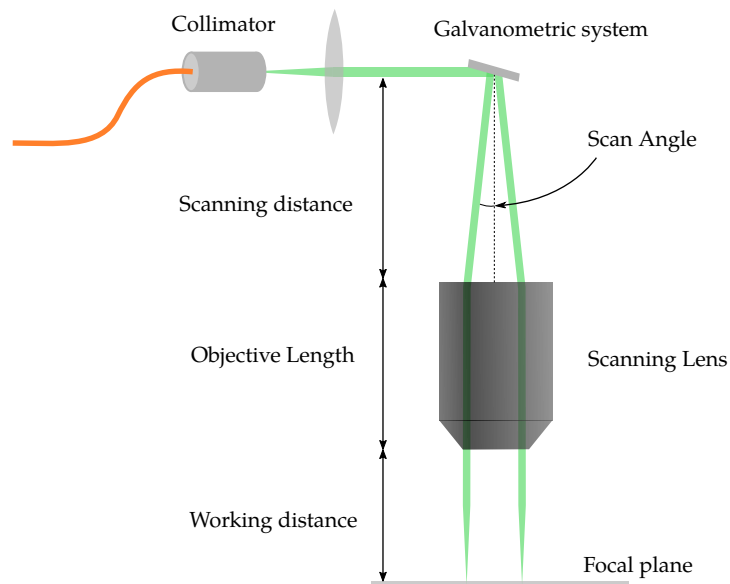


Figure 4.3: Basic diagram of a SS-OCT setup

4.3.4 Axial Measurements

4.3.5 Amplified Photodiode

Content

4.4 GALVANOMETRIC SYSTEM CONTROL

1. NI-DAQmx framework
2. C programming
3. Triggering and Clocking
4. Splitting Positive and Negative voltages
5. Conversion from volts to angles to surface area
6. Trigger enable
7. X-Motor -> Triangle Wave
8. Y-Motor -> Staircase for C-scans

4.5 USAF TARGET

1. What it is
2. How it works

¹ <http://www.openmp.org/>

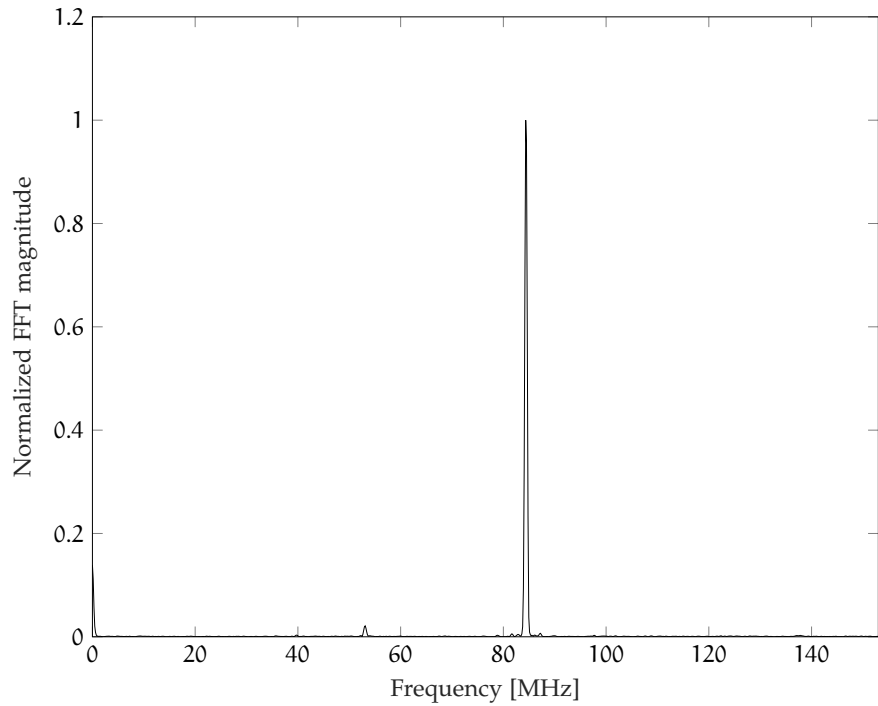


Figure 4.4: Beat frequency generated by the unbalanced MZI!, sampled with the internal 500MS/s clock.

3. Acquisitions in different conditions
4. B-scans
5. Surface images -> verifying transverse resolution

Content

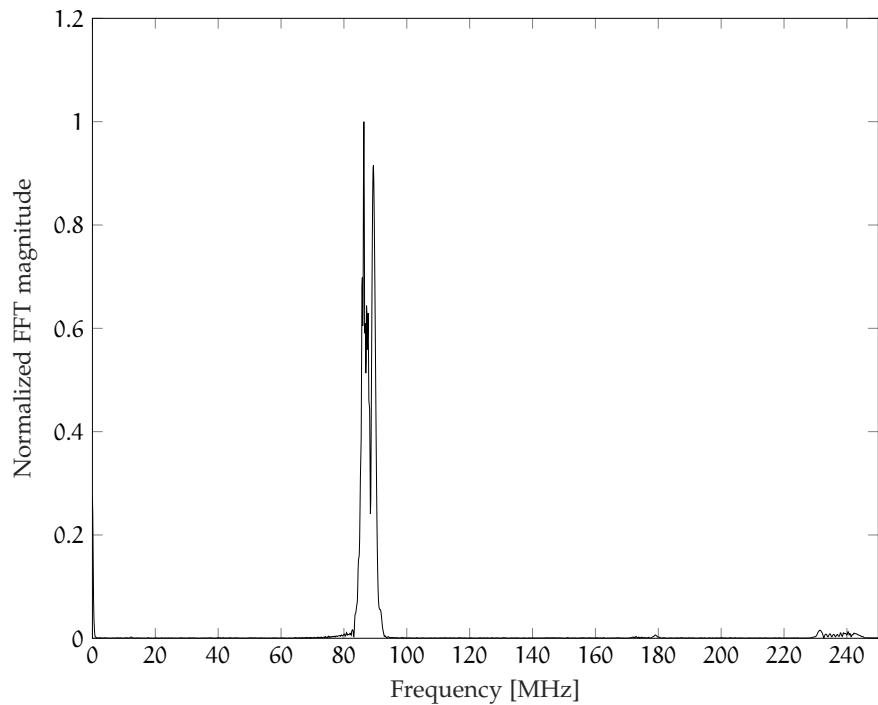


Figure 4.5: Beat frequency generated by the unbalanced MZI!, sampled with the external k-clock.

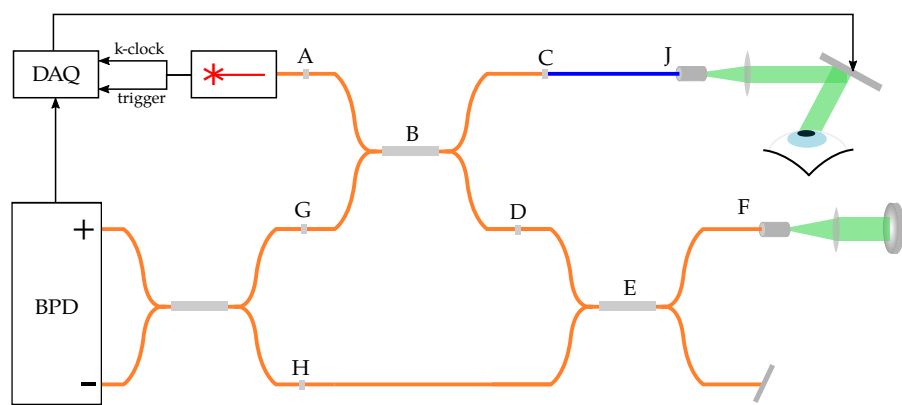


Figure 4.6: Final SS-OCT setup.

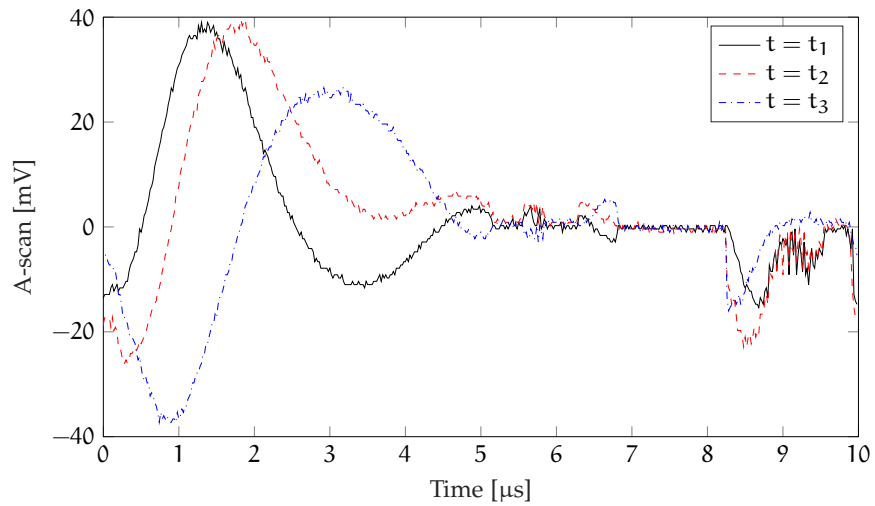


Figure 4.7: Time signal when the optical path difference is close to 0.

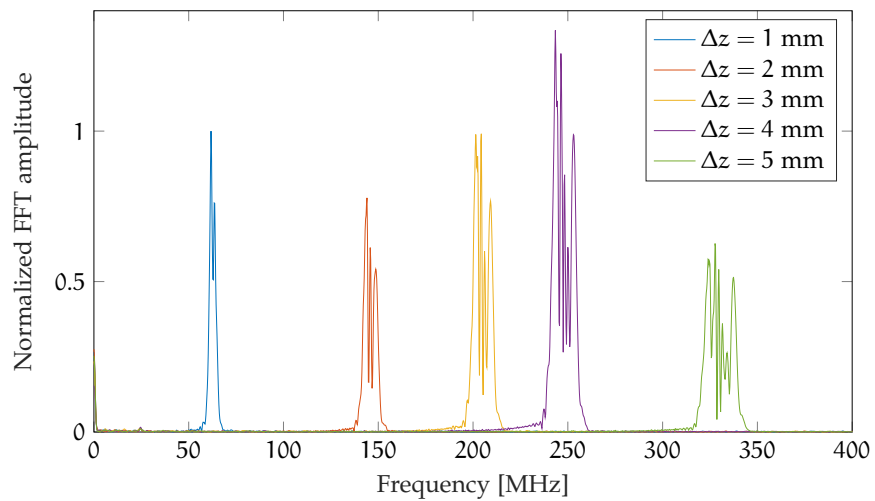


Figure 4.8: Effect of reference arm unbalancing on the beat frequency

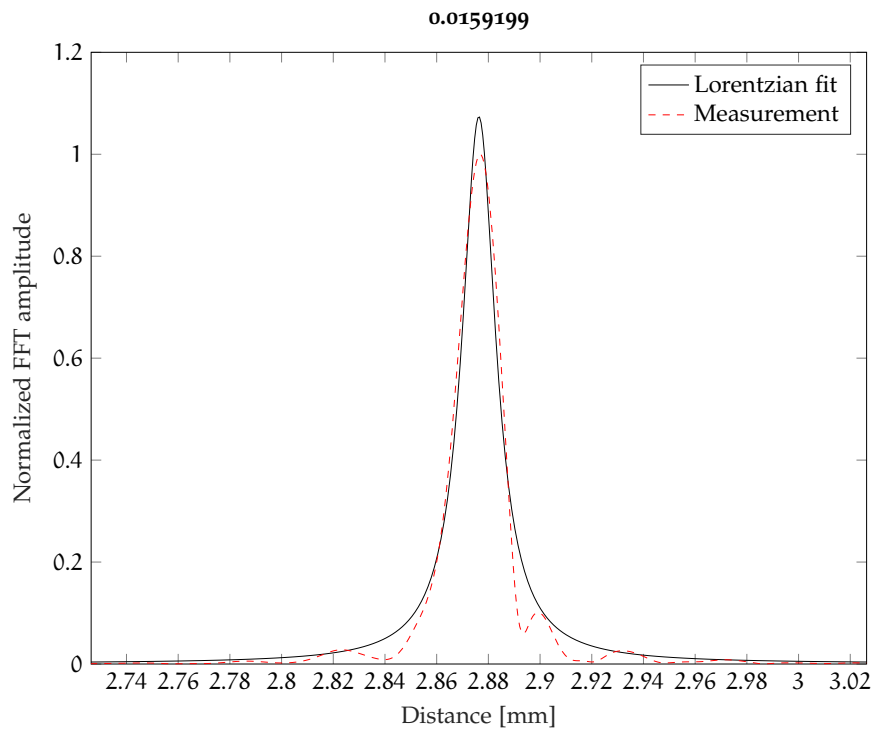


Figure 4.9: Estimate of the axial resolution with Lorentzian curve fitting.
 Nonlinear least squares. $y_0 = 0.0009$, $x_c = 2.8763$, $A = 0.0268$,
 $w = 0.0159$

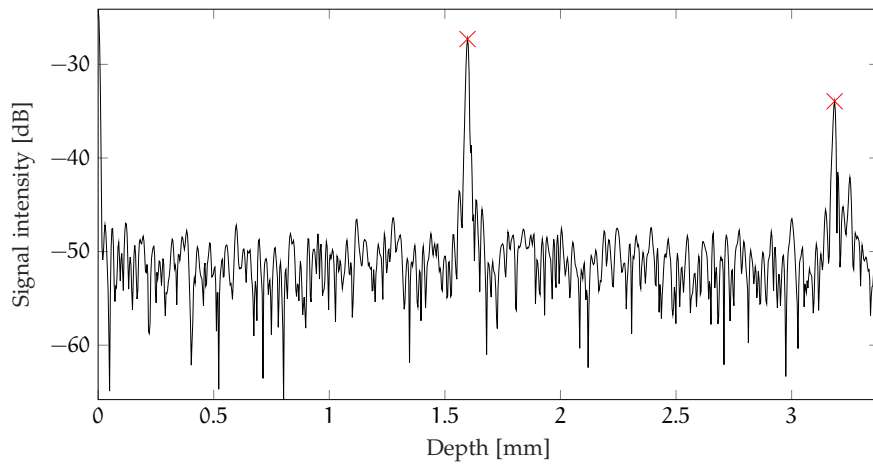


Figure 4.10: Axial measurement of the USAF target.

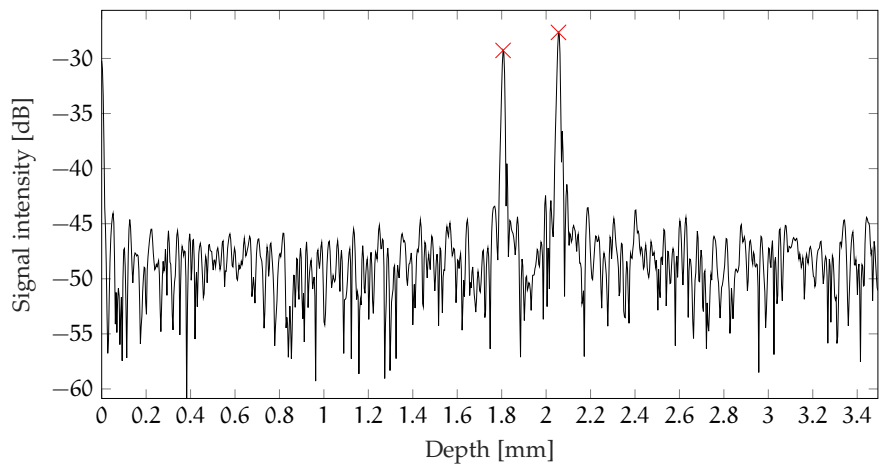


Figure 4.11: Axial measurement of an optical fiber.

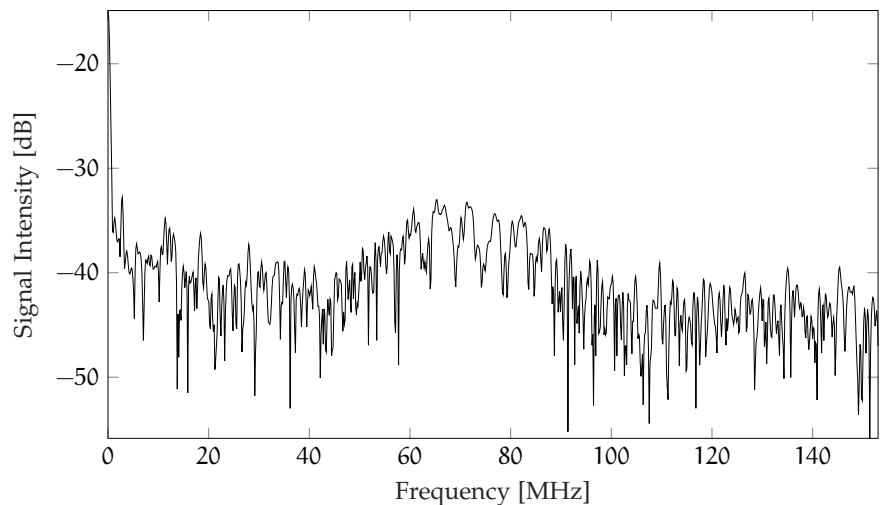


Figure 4.12: Spurious beat frequencies detected by the Exalos BPD!.

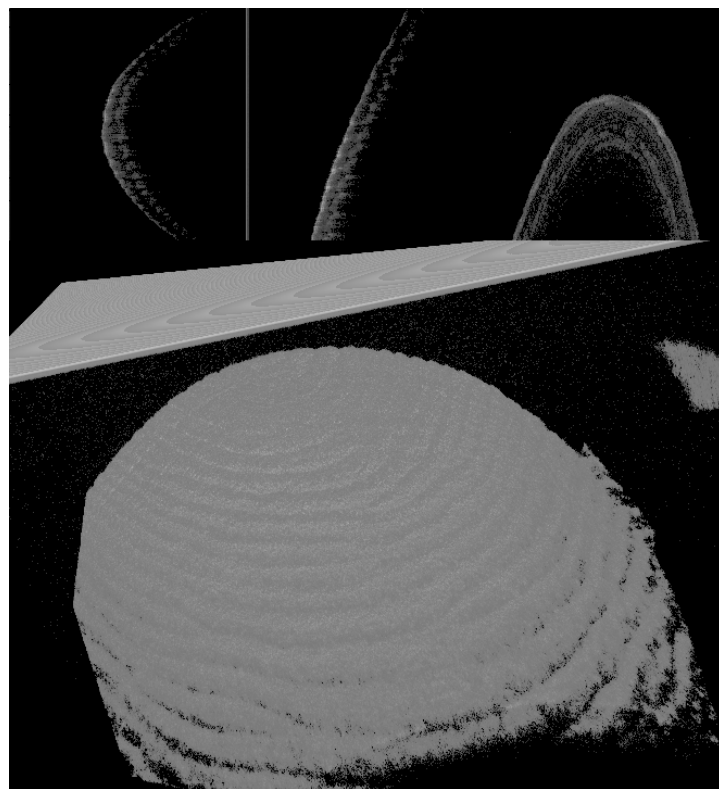


Figure 4.13: 3D rendering of a human finger.

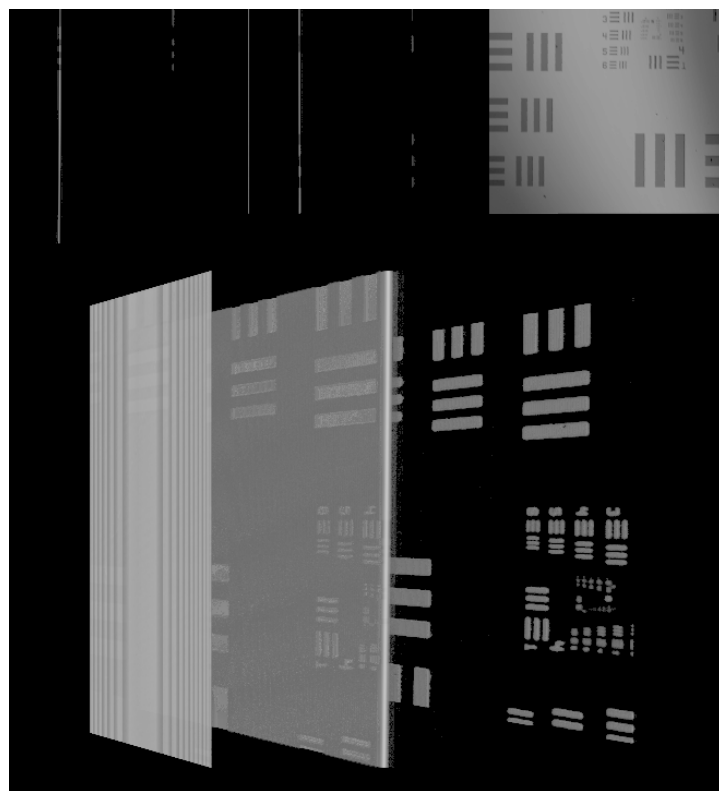


Figure 4.14: 3D rendering of the USAF target

5

CONCLUSIONS

Part I
APPENDIX

A

APPENDIX TEST

A.1 APPENDIX SECTION TEST

More dummy text

A.2 ANOTHER APPENDIX SECTION TEST

Donec et nisl at wisi luctus bibendum. Nam interdum tellus ac libero. Sed sem justo, laoreet vitae, fringilla at, adipiscing ut, nibh. Maecenas non sem quis tortor eleifend fermentum. Etiam id tortor ac mauris porta vulputate. Integer porta neque vitae massa. Maecenas tempus libero a libero posuere dictum. Vestibulum ante ipsum primis in faucibus orci luctus et ultrices posuere cubilia Curae; Aenean quis mauris sed elit commodo placerat. Class aptent taciti sociosqu ad litora torquent per conubia nostra, per inceptos hymenaeos. Vivamus rhoncus tincidunt libero. Etiam elementum pretium justo. Vivamus est. Morbi a tellus eget pede tristique commodo. Nulla nisl. Vestibulum sed nisl eu sapien cursus rutrum.

There is also a useless Pascal listing below: ??.

LABITUR BONORUM PRI NO	QUE VISTA	HUMAN
fastidii ea ius	germano	demonstratea
suscipit instructior	titulo	personas
quaestio philosophia	facto	demonstrated

Table A.1: Autem usu id.

BIBLIOGRAPHY

- [1] B. T. Amaechi, S. M. Higham, A. GH. Podoleanu, J. A. Rogers, and D. A. Jackson. "Use of optical coherence tomography for assessment of dental caries: quantitative procedure." In: *Journal of Oral Rehabilitation* 28.12 (2001), pp. 1092–1093. ISSN: 0305-182X. DOI: [10.1046/j.1365-2842.2001.00840.x](https://doi.wiley.com/10.1046/j.1365-2842.2001.00840.x). URL: <http://doi.wiley.com/10.1046/j.1365-2842.2001.00840.x>.
- [2] Oscar Barajas, Amir Tofighi Zavareh, and Sebastian Hoyos. "Towards an on-chip signal processing solution for the online calibration of SS-OCT systems." In: *2017 IEEE International Symposium on Circuits and Systems (ISCAS)*. IEEE, 2017, pp. 1–4. ISBN: 978-1-4673-6853-7. DOI: [10.1109/ISCAS.2017.8050241](https://ieeexplore.ieee.org/document/8050241/). URL: <http://ieeexplore.ieee.org/document/8050241/>.
- [3] Max Born, Emil Wolf, A. B. Bhatia, P. C. Clemmow, D. Gabor, A. R. Stokes, A. M. Taylor, P. A. Wayman, and W. L. Wilcock. *Principles of Optics: Electromagnetic Theory of Propagation, Interference and Diffraction of Light*. 7th ed. Cambridge University Press, 1999. DOI: [10.1017/CBO9781139644181](https://doi.org/10.1017/CBO9781139644181).
- [4] B E Bouma et al. "Evaluation of intracoronary stenting by intravascular optical coherence tomography." In: *Heart* 89.3 (2003), pp. 317–320. ISSN: 1355-6037. DOI: [10.1136/heart.89.3.317](https://doi.org/10.1136/heart.89.3.317). eprint: [http://heart.bmjjournals.org/content/89/3/317.full.pdf](https://heart.bmjjournals.org/content/89/3/317.full.pdf). URL: [http://heart.bmjjournals.org/content/89/3/317](https://heart.bmjjournals.org/content/89/3/317).
- [5] Marco Calabrese. "Progetto di un Tomografo a Coerenza Ottica ad Alta Velocità." MA thesis. Dipartimento di Ingegneria dell'Informazione, Padova (Italy): Università degli Studi di Padova, 2017.
- [6] Dong-hak Choi, Hideaki Hiro-Oka, Kimiya Shimizu, and Kohji Ohbayashi. "Spectral domain optical coherence tomography of multi-MHz A-scan rates at 1310 nm range and real-time 4D-display up to 41 volumes/second." In: *Biomedical Optics Express* 3.12 (2012), p. 3067. ISSN: 2156-7085. DOI: [10.1364/BOE.3.003067](https://doi.org/10.1364/BOE.3.003067). URL: <https://www.osapublishing.org/abstract.cfm?URI=boe-3-12-3067>.
- [7] Seyed Hamid Hosseiny Darbazi. "GPU-Accelerated Optical Coherence Tomography Signal Processing and Visualization." PhD thesis. Universidade do Porto, 2016.
- [8] Al-Hafeez Dhalla, Derek Nankivil, and Joseph a. Izatt. "Complex conjugate resolved heterodyne swept source optical coherence tomography using coherence revival." In: *Biomedical Optics*

- Express* 3.3 (2012), p. 633. ISSN: 2156-7085. DOI: [10.1364/B0E.3.000633](https://doi.org/10.1364/B0E.3.000633).
- [9] Wolfgang Drexler and James G. Fujimoto, eds. *Optical Coherence Tomography*. Cham: Springer International Publishing, 2015. ISBN: 978-3-319-06418-5. DOI: [10.1007/978-3-319-06419-2](https://doi.org/10.1007/978-3-319-06419-2). URL: <http://link.springer.com/10.1007/978-3-319-06419-2>.
 - [10] P. F. Escobar, J. L. Belinson, A. White, N. M. Shakhova, F. I. Feldchtein, M. V. Kareta, and N. D. Gladkova. "Diagnostic efficacy of optical coherence tomography in the management of preinvasive and invasive cancer of uterine cervix and vulva." In: *International Journal of Gynecological Cancer* 14.3 (2004), pp. 470–474. ISSN: 1048-891X. DOI: [10.1111/j.1048-891x.2004.14307.x](https://doi.org/10.1111/j.1048-891x.2004.14307.x). URL: <http://doi.wiley.com/10.1111/j.1048-891x.2004.14307.x>.
 - [11] J G Fujimoto, C a Puliafito, R Margolis, A Oseroff, S De Silvestri, and E P Ippen. "Femtosecond optical ranging in biological systems." In: *Optics Letters* 11.3 (1986), p. 150. ISSN: 0146-9592. DOI: [10.1364/OL.11.000150](https://doi.org/10.1364/OL.11.000150). URL: <https://www.osapublishing.org/abstract.cfm?URI=ol-11-3-150>.
 - [12] T GAMBICHLER, G MOUSSA, M SAND, D SAND, P ALTMAYER, and K HOFFMANN. "Applications of optical coherence tomography in dermatology." In: *Journal of Dermatological Science* 40.2 (2005), pp. 85–94. ISSN: 09231811. DOI: [10.1016/j.jdermsci.2005.07.006](https://doi.org/10.1016/j.jdermsci.2005.07.006). URL: <http://linkinghub.elsevier.com/retrieve/pii/S092318110500201X>.
 - [13] Alexandre R. Hariri Lidaand Tumlinson, David G. Besselsen, Urs Utzinger, Eugene W. Gerner, and Jennifer K. Barton. "Endoscopic optical coherence tomography and laser-induced fluorescence spectroscopy in a murine colon cancer model." In: *Lasers in Surgery and Medicine* 38.4 (2006), pp. 305–313. ISSN: 0196-8092. DOI: [10.1002/lsm.20305](https://doi.org/10.1002/lsm.20305). URL: <http://doi.wiley.com/10.1002/lsm.20305>.
 - [14] David Huang et al. "Optical Coherence Tomography HHS Public Access." In: *Science. November* 22.2545035 (1991), pp. 1178–1181. ISSN: 0036-8075. DOI: [10.1126/science.22.2545035](https://doi.org/10.1126/science.22.2545035). arXiv: [15334406](https://arxiv.org/abs/15334406).
 - [15] Ik-Kyung Jang et al. "Visualization of coronary atherosclerotic plaques in patients using optical coherence tomography: comparison with intravascular ultrasound." In: *Journal of the American College of Cardiology* 39.4 (2002), pp. 604–609. ISSN: 0735-1097. DOI: [10.1016/S0735-1097\(01\)01799-5](https://doi.org/10.1016/S0735-1097(01)01799-5). eprint: <http://www.onlinejacc.org/content/39/4/604.full.pdf>. URL: <http://www.onlinejacc.org/content/39/4/604>.

- [16] Yali Jia et al. "Quantitative Optical Coherence Tomography Angiography of Choroidal Neovascularization in Age-Related Macular Degeneration." In: *Ophthalmology* 121.7 (2014), pp. 1435–1444. ISSN: 01616420. DOI: [10.1016/j.ophtha.2014.01.034](https://doi.org/10.1016/j.ophtha.2014.01.034). URL: <http://linkinghub.elsevier.com/retrieve/pii/S0161642014001043>.
- [17] Vrushali R. Korde et al. "Using optical coherence tomography to evaluate skin sun damage and precancer." In: *Lasers in Surgery and Medicine* 39.9 (2007), pp. 687–695. ISSN: 01968092. DOI: [10.1002/lsm.20573](https://doi.org/10.1002/lsm.20573). arXiv: [NIHMS150003](https://arxiv.org/abs/1500.03).
- [18] Kenneth K. C. Lee, Adrian Mariampillai, Joe X. Z. Yu, David W. Cadotte, Brian C. Wilson, Beau a. Standish, and Victor X. D. Yang. "Real-time speckle variance swept-source optical coherence tomography using a graphics processing unit." In: *Biomedical Optics Express* 3.7 (2012), p. 1557. ISSN: 2156-7085. DOI: [10.1364/BOE.3.001557](https://doi.org/10.1364/BOE.3.001557).
- [19] Wenchao Liao, Tianyuan Chen, Chengming Wang, Wenxin Zhang, Zhangkai Peng, Xiao Zhang, Shengnan Ai, Deyong Fu, Tieying Zhou, and Ping Xue. "Endoscopic optical coherence tomography with a focus-adjustable probe." In: *Optics Letters* 42.20 (2017), p. 4040. ISSN: 0146-9592. DOI: [10.1364/OL.42.004040](https://doi.org/10.1364/OL.42.004040). URL: <https://www.osapublishing.org/abstract.cfm?URI=ol-42-20-4040>.
- [20] Monika Machoy, Julia Seeliger, Liliana Szyszka-Sommerfeld, Robert Koprowski, Tomasz Gedrange, and Krzysztof Woźniak. "The Use of Optical Coherence Tomography in Dental Diagnostics: A State-of-the-Art Review." In: *Journal of Healthcare Engineering* 2017 (2017). ISSN: 20402309. DOI: [10.1155/2017/7560645](https://doi.org/10.1155/2017/7560645).
- [21] Carlo G. Someda. *Electromagnetic Waves*. 2nd ed. CRC, 2006.
- [22] Richard F. Spaide, James M. Klancnik, and Michael J. Cooney. "Retinal Vascular Layers Imaged by Fluorescein Angiography and Optical Coherence Tomography Angiography." In: *JAMA Ophthalmology* 133.1 (2015), p. 45. ISSN: 2168-6165. DOI: [10.1001/jamaophthalmol.2014.3616](https://doi.org/10.1001/jamaophthalmol.2014.3616). URL: <http://archopht.jamanetwork.com/article.aspx?doi=10.1001/jamaophthalmol.2014.3616>.
- [23] G. J. Tearney, S. A. Boppart, B. E. Bouma, M. E. Brezinski, N. J. Weissman, J. F. Southern, and J. G. Fujimoto. "Scanning single-mode fiber optic catheter-endoscope for optical coherence tomography." In: *Opt. Lett.* 21.7 (1996), pp. 543–545. DOI: [10.1364/OL.21.000543](https://doi.org/10.1364/OL.21.000543). URL: <http://ol.osa.org/abstract.cfm?URI=ol-21-7-543>.
- [24] Wolfgang Wieser, Wolfgang Draxinger, Thomas Klein, Sebastian Karpf, Tom Pfeiffer, and Robert Huber. "High definition live 3D-OCT in vivo: design and evaluation of a 4D OCT engine with 1 GVoxel/s." In: *Biomed. Opt. Express* 5.9 (2014), pp. 2963–

2977. DOI: [10.1364/BOE.5.002963](https://doi.org/10.1364/BOE.5.002963). URL: <http://www.osapublishing.org/boe/abstract.cfm?URI=boe-5-9-2963>.
- [25] Tuqiang Xie, Huikai Xie, Gary K. Fedder, and Yingtian Pan. "Endoscopic optical coherence tomography with a modified microelectromechanical systems mirror for detection of bladder cancers." In: *Applied Optics* 42.31 (2003), p. 6422. ISSN: 0003-6935. DOI: [10.1364/AO.42.006422](https://doi.org/10.1364/AO.42.006422). URL: [https://www.osapublishing.org/abstract.cfm?URI=ao-42-31-6422](http://www.osapublishing.org/abstract.cfm?URI=ao-42-31-6422).
- [26] Kang Zhang and Jin U. Kang. "Real-time 4D signal processing and visualization using graphics processing unit on a regular nonlinear-k Fourier-domain OCT system." In: *Opt. Express* 18.11 (2010), pp. 11772–11784. DOI: [10.1364/OE.18.011772](https://doi.org/10.1364/OE.18.011772). URL: <http://www.opticsexpress.org/abstract.cfm?URI=oe-18-11-11772>.